OPEN ACCESS
JOURNAL OF ADVANCED DIELECTRICS
Vol. 12, No. 5 (2022) 2244006 (7 pages)

DOI: 10.1142/S2010135X22440064

Enhanced piezoelectric properties and temperature stability in KNN-based textured ceramics

Yan Lin, Ru Wang, Jiawei Qu, Shuo Gao, Yi Zhang, Junli Yan, Jigong Hao, Peng Li* and Wei Li

School of Materials Science and Engineering, Liaocheng University
Liaocheng 252059, P. R. China

*leepeng0124@163.com

Received 27 June 2022; Revised 7 September 2022; Accepted 14 September 2022; Published 26 October 2022

Considering the advantages of high Curie temperature and environment-friendly nature of KNN piezoelectric ceramics, the limitation of weak piezoelectric response and their temperature sensitivity to applications is worth exploring. Herein, the <001> textured (1-x)($K_{0.5}Na_{0.5}$)($Nb_{0.96}Sb_{0.04}$)O_3-x($Bi_{0.5}Na_{0.5}$)HfO_3 (x = 0.01–0.045) lead-free ceramics were synthesized by templated grain-growth method. The high piezoelectric performance (d_{33} of 474 pC/N and strain of 0.21%) and excellent temperature stability (unipolar strain maintained within 4.3% change between 30°C and 165°C) were simultaneously achieved in the textured KNNS-0.03BNH ceramics. The high piezoelectric performance can be attributed to the summation of the crystallographic anisotropy and phase structure contributions in <001> textured ceramics. The superior temperature stability of piezoelectric properties can be interpreted by the contribution of crystal anisotropy to piezoelectric properties reduces the effect of phase transition on piezoelectric properties deterioration. This study provides an effective strategy for simultaneously achieving high piezoelectric properties and superior temperature stability in KNN-based textured ceramics.

Keywords: Textured ceramics; phase structure; piezoelectric properties; temperature stability.

1. Introduction

Piezoelectric ceramics are widely utilized in sensors, transducers and actuators because of their electromechanical conversion properties.[1] Lead-containing piezoelectric ceramics represented by Pb(Zr, Ti)O_3 (PZT) have been the mainstay of the piezoelectric materials market for decades owing to their superior piezoelectric properties and thermal stability.[2–4] However, in the face of the serious situation in which the toxicity of lead poses a significant risk to the environment, researchers have devoted tremendous efforts to lead-free piezoelectric ceramics. In recent years, $BaTiO_3$ (BT), ($Bi_{0.5}Na_{0.5}$)TiO_3 (BNT) and (K, Na) NbO_3 (KNN)-based piezoelectric materials have received extensive attention,[5–9] KNN-based piezoelectric materials are considered as a promising alternative to PZT systems because of their good piezoelectric response and high Curie temperature through phase structure modification.

To meet the requirements of practical applications, the lead-free ceramic systems are modified by chemical doping to improve their electrical properties. For KNN-based ceramics, the phase structure regulation by composition modification has been confirmed to be an effective strategy. It is reported that the material components at the polymorphic phase boundary usually have a lower free energy, which is favorable for polarization reversion of domains and thus the enhancement of piezoelectric and dielectric properties in KNN-based ceramics.[10–12] At present, there are four phase boundaries of KNN-based piezoelectric ceramics at room temperature, namely R–O, O–T, R–T and R–O–T.[13–15] Polymorphic phase boundaries have been achieved by doping chemical elements Sb, Ta and Li^+ or second end members, e.g., $BaZrO_3$, $CaZrO_3$ and $SrZrO_3$, etc.[16–20] Based on this strategy, Wang reported the ($Na_{0.52}K_{0.435}Li_{0.045}$)($Nb_{0.905}Sb_{0.045}Ta_{0.05}$)$O_3$ lead-free piezoelectric ceramics with O–T phase coexistence, which show a high piezoelectric response of d_{33}~308 pC/N, and an electromechanical coupling coefficient k_p up to 51%.[21] Wu and Tao *et al*. synthesized the KNN-based piezoelectric ceramics with R–O–T phase boundaries at room temperature by regulating the chemical component in the KNNS-BNKZ-Fe-xAS system. The optimal piezoelectric constant d_{33} is up to 650 pC/N, which is comparable to that of commercial PZT-based piezoelectric ceramics.[22]

In addition to the strategy of phase structure modification, crystal orientation is also an effective method for enhancing the electrical properties of KNN-based piezoelectric ceramics by taking advantage of the strong anisotropy of crystals.[23–25]

*Corresponding author.

For example, Saito *et al*. reported that d_{33} as high as 416 pC/N was achieved in <00l> textured KNN-based ceramics doped with Li, Ta and Sb.[26] Li prepared 0.96KNNS–0.01CZ–0.03BKH textured ceramics characterized with R–O phase structure, and an ultrahigh d_{33} of ~700 pC/N was obtained in these ceramics.[27] In this study, the (1-*x*)-$(K_{0.5}Na_{0.5})(Nb_{0.96}Sb_{0.04})O_3$-*x*$(Bi_{0.5}Na_{0.5})HfO_3$ (x = 0.01, 0.02, 0.03, 0.04 and 0.045) textured ceramics and their random counterparts have been synthesized. Superior piezoelectric properties (d_{33} of 474pC/N, strain of 0.21% at 40 kV/cm) and good temperature stability of a relatively low strain deviation of 4.3% between 30°C and 165°C were achieved in the KNNS-0.03BNH textured ceramics.

2. Experimental Section

<00l> textured (1-*x*)$(K_{0.5}Na_{0.5})(Nb_{0.96}Sb_{0.04})O_3$-*x*$(Bi_{0.5}Na_{0.5})HfO_3$ ceramics was prepared by template grain growth (TGG) method. The platelet-like $NaNbO_3$ seed crystals with a high aspect ratio was used as templates to induce crystal orientation in the matrix. Raw materials including K_2CO_3 (99%), Na_2CO_3 (99.95%), Nb_2O_5 (99.98%), Sb_2O_3 (99.99%), Bi_2O_3 (99%) and HfO_2 (99.99%) were weighed according to the stoichiometry and then ball-milled for 18 h. After the slurries were dried, the powders were calcined at 850°C for 5 h. Subsequently, the calcined powders were ball-milled for 60 h, dried at 100°C and homogenized using a screen mesh with an aperture size of 0.075 μm. The templates for texturing KNNS–BNH ceramics are plate-like <001>-oriented $NaNbO_3$ microcrystals. The <001>-oriented $NaNbO_3$ templates were synthesized by topochemical microcrystal conversion method. In the first step, the precursor $Bi_{2.5}Na_{3.5}Nb_5O_{18}$ was synthesized in NaCl molten salt using Bi_2O_3, Na_2CO_3 and Nb_2O_5 as raw materials. In the next step, $Bi_{2.5}Na_{3.5}Nb_5O_{18}$ precursor was mixed with Na_2CO_3 and NaCl salt, and then heated to 970°C for 2 h. Bi^{3+} in $Bi_{2.5}Na_{3.5}Nb_5O_{18}$ was substituted by the Na^+ from Na_2CO_3, yielding $NaNbO_3$ templates and Bi_2O_3 byproduct. The Bi_2O_3 byproduct was removed by diluted nitric acid. To fabricate tape-casting slurries, the KNNS–BNH matrix powders, $NaNbO_3$ templates and binder were mixed in a solvent (75 wt.% alcohol and 25 wt.% toluene) for 10 h. The slurries were cast on glass to form tapes. The dried tapes were stacked and pressed under 20 MPa at 65°C for 20 min. After the organic binder was removed, the green samples were sintered using a two-step process. The samples were sintered using a two-step sintering process (T_1= 1190°C for 0 min followed by T_2 = 1090°C for 6 h) to ensure adequate epitaxial growth of grains.

The room temperature phase structure was characterized by X-ray diffraction (XRD, D/MAX 2550 V, Rigaku, Japan). The temperature-dependent dielectric properties were measured using an LCR meter (E4980A, Agilent). The microstructure was observed using a field emission scanning electron microscope (FE-SEM, Carl Zeiss, Merlin Compact). Polarization hysteresis, unipolar strain curves and temperature dependence of unipolar strain curves were measured by a ferroelectric test system (aix-ACCT TF Analyzer 3000, Germany). After the ceramics were poled under an electric field of 20 kV/cm for 30 min, the piezoelectric coefficient d_{33} was tested using a quasi-static d_{33} meter (YE2730A, China).

3. Results and Discussion

Figure 1 shows the XRD patterns of KNNS–*x*BNH (x = 0.01–0.045) textured and random ceramics, measured in the 2θ range of 20–60° at room temperature. The intensities of the (001) and (002) peaks of textured ceramics were significantly higher than those of the random counterparts, indicating most of the crystals grow preferentially along the crystallographic direction of [001]. The degree of texturing was determined by Lotgering factor $F_{(001)}$. The Lotgering factor $F_{(001)}$ is defined as the intensity fraction of preferred crystallographic orientation by the following equations:

$$F_{(001)} = \frac{P_{(00l)} - P_0}{1 - P_0}, \quad (1)$$

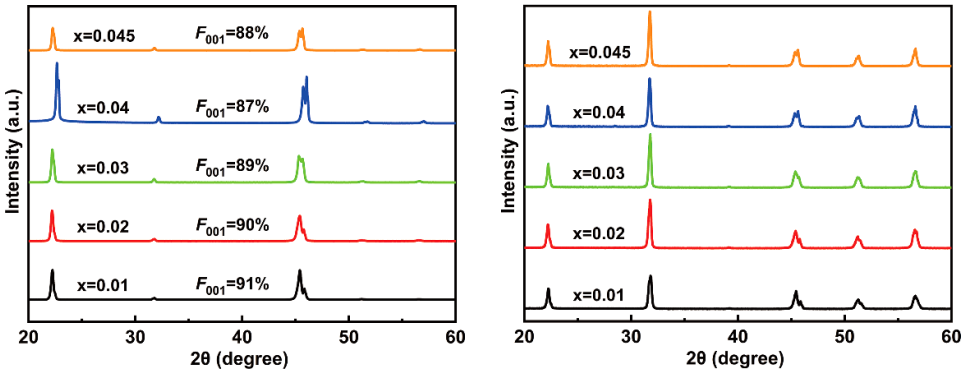

Fig. 1. (a) XRD patterns of KNNS-*x*BNH (x = 0.01, 0.02, 0.03, 0.04 and 0.045) textured ceramics (a) and random ceramics (b) in the 2θ range of 20°–60°.

$$P_{(00l)} = \frac{\sum I_{(00l)}}{\sum I_{(hkl)}}, \quad (2)$$

$$P_0 = \frac{\sum I_{0(00l)}}{\sum I_{0(hkl)}}, \quad (3)$$

where $I_{(hkl)}$ and $I_{0(hkl)}$ are XRD intensities of all the (hkl) diffraction peaks in the textured and random ceramics, respectively. While $I_{(00l)}$ and $I_{0(hkl)}$ are the XRD intensities of all the (001) peaks in the textured and random ceramics.

The texturing degrees $F_{(00l)}$ of x = 0.01–0.045 textured ceramics calculated by Lotgering's method are 91%, 90%, 89%, 87% and 88%, respectively.[4,28] The phase structure of KNNS–xBNH textured ceramics can be determined by the relative strength of the (002) and (200) peaks.[29,30] For the KNNS–xBNH textured ceramics with x = 0.01 and 0.02, the intensity of (002) peak is nearly twice that of (200), indicating that the structure is dominated by orthorhombic (O) phase at room temperature. For the textured ceramics with x = 0.03, 0.04 and 0.045, the strength ratios of I_{002}/I_{200} are all less than 1:1, indicating that the ceramics exhibit multiphase coexistence at room temperature. To further determine the phase transition process of KNNS–xBNH textured ceramics, the ε_r-T curves were measured in the temperature range of 20–480°C, as shown in Fig. 2. With increasing BNH content, the orthogonal–tetragonal phase transition temperature (T_{O-T}) gradually decreased to room temperature. Combined with the XRD analysis, the phase structure of the textured ceramics with x = 0.03 is supposed to be R–O–T multiphase coexistence, while the ceramics with x = 0.04 and 0.045 are R and T coexisted phase structures.

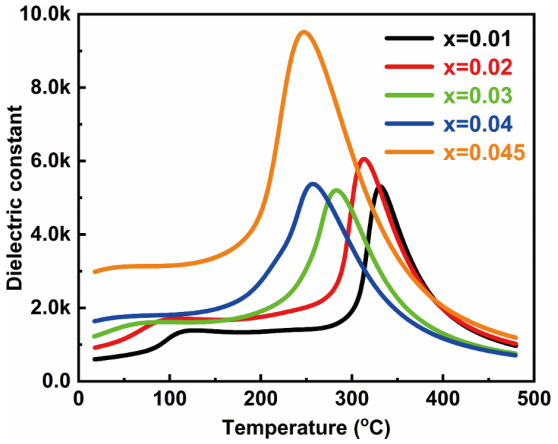

Fig. 2. ε_r-T curves of KNNS-xBNH textured ceramics measured in the temperature range of 20–480°C.

The cross-sectional SEM images of KNNS–xBNH textured ceramics are presented in Fig. 3. It can be clearly observed that all ceramics show a dense microstructure and the cubical-shaped grains are well arranged along the crystallographic [001] direction perpendicular to the tape casting direction, which is consistent with the results revealed by XRD patterns. The XRD and SEM measurement results

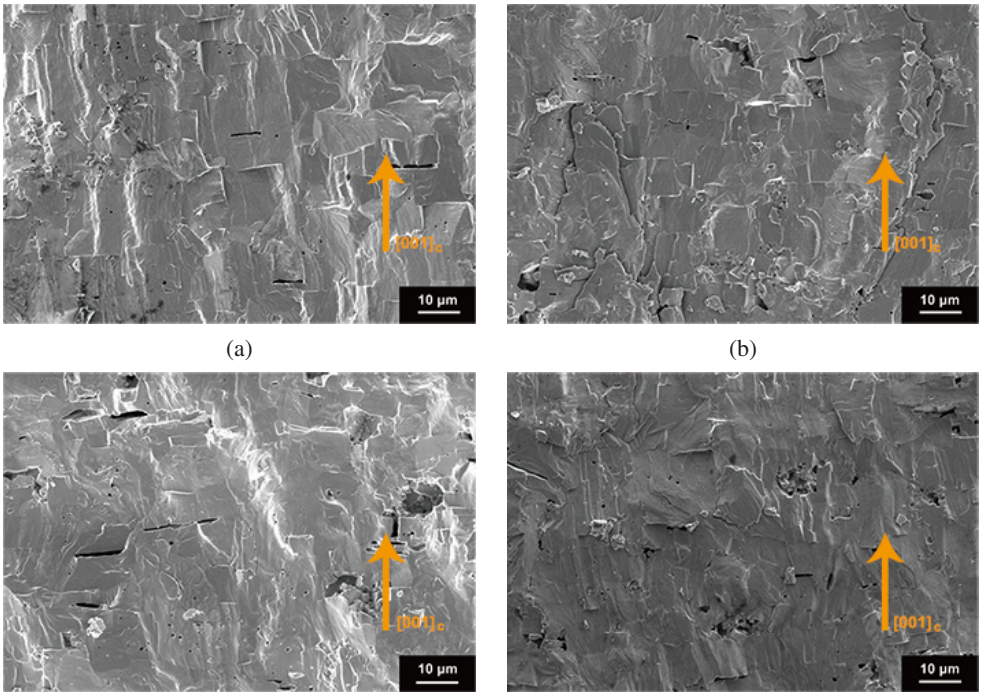

(a) (b) (c) (d)

Fig. 3. SEM images of cross section of KNNS-xBNH textured ceramics normal to the tape casting direction; (a) x = 0.01, (b) x = 0.02, (c) x = 0.03 and (d) x = 0.04.

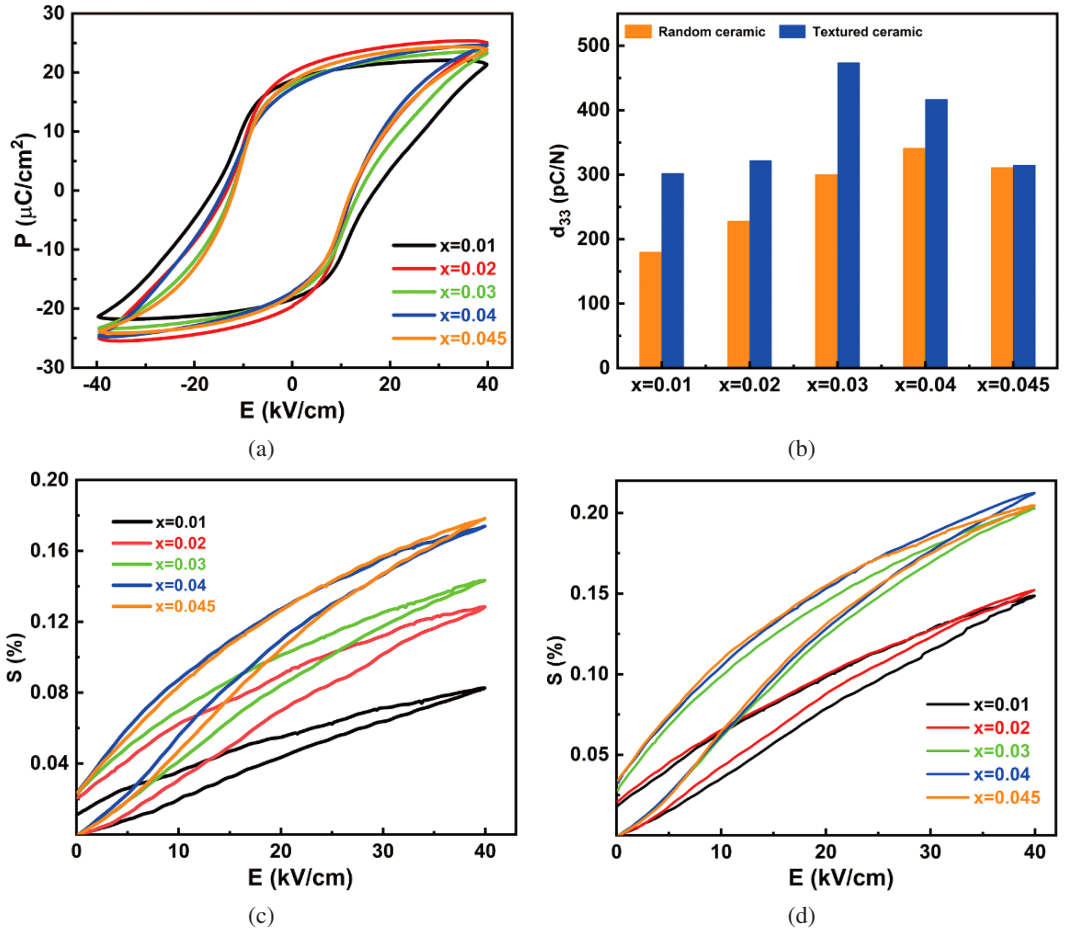

Fig. 4. (a) Polarization hysteresis (P-E) loops of KNNS-xBNH (x = 0.01, 0.02, 0.03, 0.04 and 0.045) textured ceramics; (b) d_{33} values of random and textured ceramics; electric field-induced unipolar strain curves of (c) random ceramics and (d) textured ceramics.

confirmed that the $NaNbO_3$ templates can induce grains texturing in KNN-based ceramics.

Figure 4(a) gives the ferroelectric hysteresis (P-E) loops of KNNS–xBNH textured ceramics at the electric field signal of amplitude and frequency of 40 kV/cm and 10 Hz, respectively. A series of saturated P-E loops with high rectangularity were observed in all samples, indicating superior ferroelectric properties. Furthermore, the remnant polarization had a similar magnitude of all samples, however, the coercive field gradually decreases with increasing BNH concentration. Figure 4(b) shows the d_{33} values of KNNS–xBNH textured ceramics and their random counterparts. One can see that the textured ceramics exhibited superior piezoresponse as compared to their random counterparts but the degree of enhancement depends on their phase structures. It is worth noting here that a high d_{33} of 474 pC/N was achieved in the KNNS–BNH textured ceramics with x = 0.03, which shows an improvement of approximately 60% as compared to their nontextured counterparts. This result implies that some inherent mechanism is responsible for the enhancement in piezoelectric properties of KNN-based systems. The superior piezoresponse in KNNS-0.03BNH textured ceramics could be understood as a combined contribution of crystallographic anisotropy and phase structure. The improvement of piezoelectric activity in textured ceramics is primarily determined by their crystallographic anisotropy nature. The improvement in the piezoelectric constant by domain engineering is much higher for <001> oriented rhombohedral and orthorhombic crystals as compared to tetragonal one with respect to $<001>_{pc}$ oriented electric field vector. Therefore, a significant improvement of longitudinal piezoelectric coefficient d_{33} shown in Fig. 4(b) was observed in the compositions containing the rhombohedral and orthorhombic phases. Apart from the piezoelectric anisotropy contribution, the phase structures also play an important role in determining the piezoelectric response in the polarization rotation ferroelectrics. The energy barrier tends to be flattened and hence the dipoles are readily switched on by applying the electric field in the composition with a coexisting multiphase. Consequently, the high piezoelectric response with d_{33} value of 474 pC/N was achieved in the <001> oriented ceramics with R–O–T coexistence. The electric field-induced strains of the random and textured KNNS–xBNH ceramics are shown in Figs. 4(c) and 4(d). It can be seen the electric

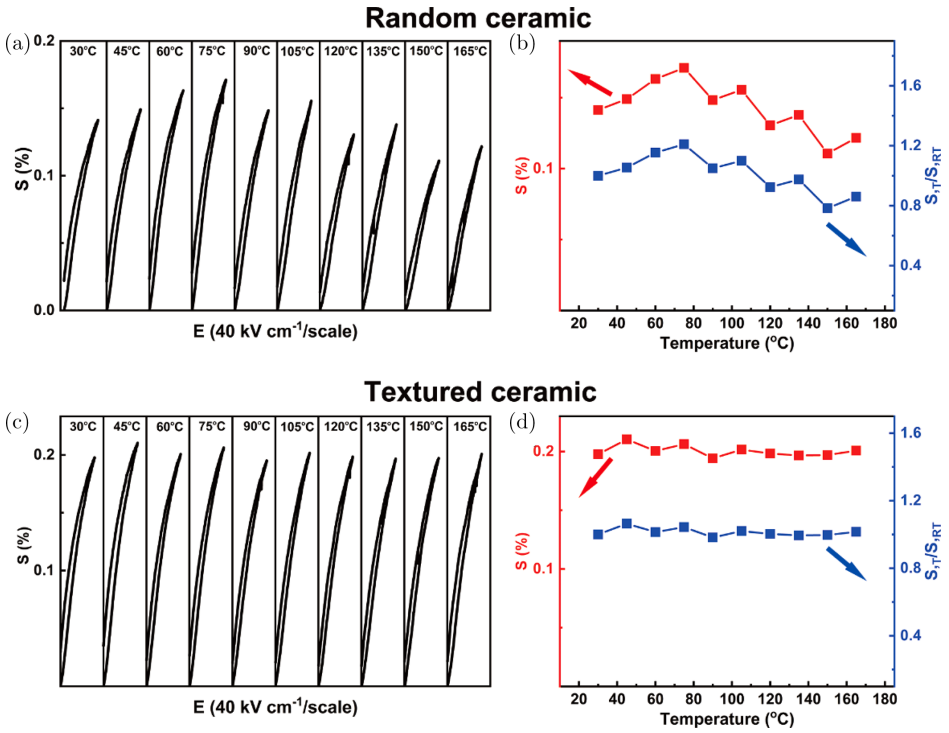

Fig. 5. Temperature dependence of unipolar strain curves of KNNS-0.03BNH random ceramics (a) and textured ceramics; (c) Temperature dependence of strain and S_T/S_{RT} values of KNNS-0.03BNH random ceramics (b) and textured ceramics (d). (S_T denotes the strain values at varied temperatures, while S_{RT} is the strain value at room temperature).

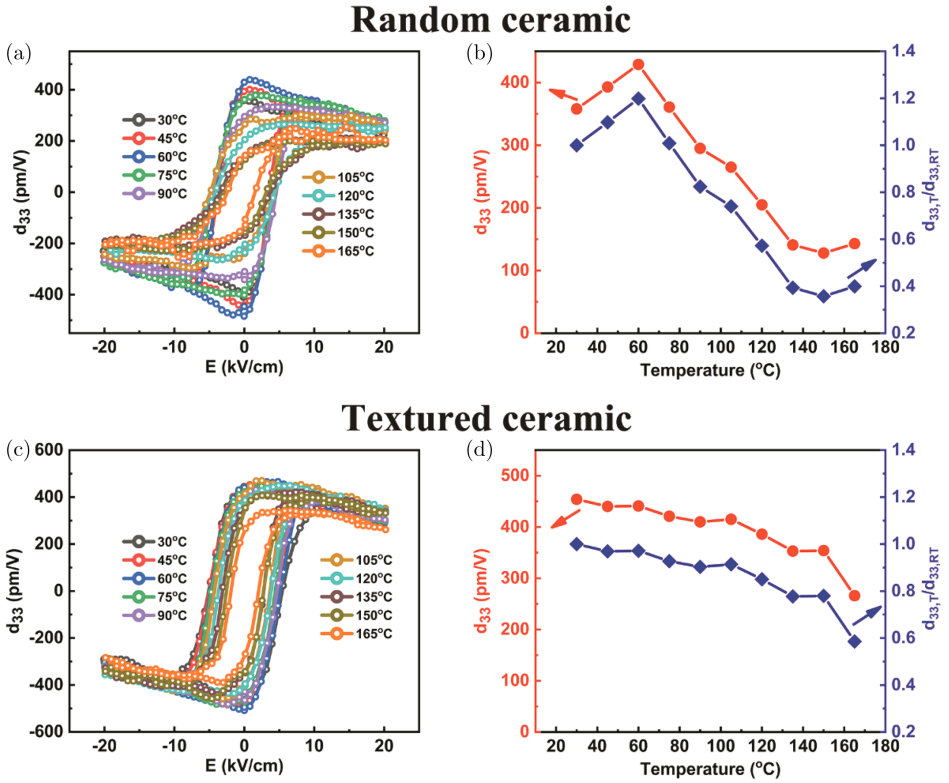

Fig. 6. Electric-field dependence of the d_{33} for the KNNS-0.03BNH random ceramics (a) and textured ceramics (c) measured at different temperatures. Temperature-dependent d_{33} and normalized d_{33} values for the KNNS-0.03BNH random ceramics (b) and textured ceramics (d).

field-induced strains of KNNS–xBNH (x = 0.01–0.045) textured ceramics have a significant enhancement as compared to their nontextured counterparts, which could be originated from the large displacement of domain walls upon applying the electric field.[4]

From a practical application viewpoint, piezoelectric ceramics should not only exhibit outstanding piezoelectric properties but also maintain the stability with respect to temperature. The unipolar strain curves of KNNS-0.03BNH random and textured ceramics as a function of temperature from room temperature to 165°C are shown in Fig. 5. The unipolar strain of random ceramics increases gradually to a peak value at 75°C, and begins to decrease severely with further elevated temperature. It is worth noting here that the unipolar strain of textured ceramics as shown in Fig. 5(d) shows a relatively low deviation within 4.3% with respect to their room temperature values in the range of 30–165°C, demonstrating good temperature stability. Figure 6 displays the electric-field-dependent small signal piezoelectric coefficient d_{33} at different temperatures. It can be seen that the d_{33} values at $E = 0$ show a slow decrease with elevated temperatures for the KNNS-0.03 textured ceramics. Note that the d_{33} values at 165°C retained almost 60% of its room temperature values, which is superior to their random counterparts. Through comparative analysis, we deduce that the contribution of crystal anisotropy to piezoelectric properties compensates the effect of piezoelectric deterioration induced by phase transition, and thus achieving superior temperature stability of piezoresponse in textured ceramics.

4. Conclusion

In this work, **<001>** textured KNNS–xBNH ceramics were found to exhibit enhanced piezoelectric performance as compared to their random counterparts. A large d_{33} value of 474 pC/N and good temperature stability of strain with a relatively low deviation of 4.3% between 30°C and 165°C were achieved in the <001> textured KNNS-0.03BNH ceramics. The comparative analysis suggests that the enhanced piezoresponse in the <001> textured ceramics is primarily determined by their crystallographic anisotropy nature and the flattened Gibbs free energy induced by R–O–T multiphase coexistence. This work proves that high piezoelectric properties and superior temperature stability of piezoresponse can be realized by the development of <001> texturing, which benefits the practical applications of lead-free piezoelectric ceramics.

Acknowledgments

This work was supported by the National Natural Science Foundation of China (Grant No. 52102132) and the Natural Science Foundation of Shandong Province of China (Grant Nos. ZR2020QE043, ZR2020ME031and ZR2020ME033), the Innovation Team of Higher Educational Science and Technology Program of Shandong Province (Grant No. 2019KJA025). Research Foundation for the Doctoral Program of Liaocheng University (Grant No. 318051932).

References

[1]Y. Liu, Y. Chang, E. Sun, F. Li, S. Zhang, B. Yang, Y. Sun, J. Wu and W. Cao, Significantly enhanced energy-harvesting performance and superior fatigue-resistant behavior in $[001]_c$-textured $BaTiO_3$-based lead-free piezoceramics, *ACS Appl. Mater. Interf.* **10**, 31488 (2018).

[2]L. Yang, H. Huang, Z. Xi, L. Zheng, S. Xu, G. Tian, Y. Zhai, F. Guo, L. Kong, Y. Wang, W. Lu, L. Yuan, M. Zhao, H. Zheng and G. Liu, Simultaneously achieving giant piezoelectricity and record coercive field enhancement in relaxor-based ferroelectric crystals, *Nat. Commun*. **13**, 2444 (2022).

[3]L. Bian, X. Qi, K. Li, Y. Yu, L. Liu, Y. Chang, W. Cao and S. Dong, High-performance $[001]_c$-textured PNN-PZT relaxor ferroelectric ceramics for electromechanical coupling devices, *Adv. Funct. Mater*. **30**, 2001846 (2020).

[4]S. Yang, J. Li, Y. Liu, M. Wang, L. Qiao, X. Gao, Y. Chang, H. Du, Z. Xu, S. Zhang and F. Li, Textured ferroelectric ceramics with high electromechanical coupling factors over a broad temperature range, *Nat. Commun*. **12**, 1414 (2021).

[5]Q. Kou, B. Yang, Y. Sun, S. Yang, L. Liu, H. Xie, Y. Chang, S. Zhang and F. Li, Tetragonal (Ba, Ca) (Zr, Ti)O_3 textured ceramics with enhanced piezoelectric response and superior temperature stability, *J. Materiomics* **8**, 366 (2021).

[6]K. Xu, J. Li, X. Lv, J. Wu, X. Zhang, D. Xiao and J. Zhu, Superior piezoelectric properties in potassium-sodium niobate lead-free ceramics, *Adv. Mater.* **28**, 8519 (2016).

[7]J. Fu and R. Zuo, Structural evidence for the polymorphic phase boundary in (Na,K)NbO_3 based perovskites close to the rhombohedral-tetragonal phase coexistence zone, *Acta Mater*. **195**, 571 (2020).

[8]J. F. Li, K. Wang, F. Y. Zhu, L. Q. Cheng, F. Z. Yao and D. J. Green, (K,Na)NbO_3-based lead-free piezoceramics: Fundamental aspects, processing technologies, and remaining challenges, *J. Am. Ceram. Soc*. **96**, 3677 (2013).

[9]X. Liu and X. Tan, Giant strains in non-textured ($Bi_{1/2}$ $Na_{1/2}$)TiO_3-based lead-free ceramics, *Adv. Mater*. **28**, 574 (2016).

[10]X. Lv, J. Zhu, D. Xiao, X. X. Zhang and J. Wu, Emerging new phase boundary in potassium sodium-niobate based ceramics, *Chem. Soc. Rev*. **49**, 671 (2020).

[11]X. Lv, J. Zhang, Y. Liu, F. Li, X. X. Zhang and J. Wu, Synergetic contributions in phase boundary engineering to the piezoelectricity of potassium sodium niobate lead-free piezoceramics, *ACS Appl. Mater. Interf.* **12**, 39455 (2020).

[12]X. Wang, J. Wu, D. Xiao, X. Cheng, T. Zheng, X. Lou, B. Zhang and J. Zhu, New potassium-sodium niobate ceramics with a giant d_{33}, *ACS Appl. Mater. Interf.* **6**, 6177 (2014).

[13]W. Yao, J. Zhang, C. Zhou, D. Liu and W. Su, Giant piezoelectricity, rhombohedral-orthorhombic-tetragonal phase coexistence and domain configurations of (K,Na)(Nb,Sb)O_3–$BiFeO_3$–(Bi, Na)ZrO_3 ceramics, *J. Eur. Ceram. Soc*. **40**, 1223 (2020).

[14]X. Lv, J. Wu, D. Xiao, H. Tao, Y. Yuan, J. Zhu, X. Wang and X. Lou, (1-x)$(K_{0.48}Na_{0.52})(Nb_{0.95-y-z}Ta_zSb_y)O_3$−x$Bi_{0.5}(Na_{0.82}K_{0.18})_{0.5}ZrO_3$ lead-free ceramics: Composition dependence of the phase boundaries and electrical properties, *Dalton Trans*. **44**, 4440 (2015).

[15]J. Wu, H. Tao, Y. Yuan, X. Lv, X. Wang and X. Lou, Role of antimony in the phase structure and electrical properties of potassium–sodium niobate lead-free ceramics, *RSC Adv*. **5**, 14575 (2015).

[16]X. Gao, Z. Cheng, Z. Chen, Y. Liu, X. Meng, X. Zhang, J. Wang, Q. Guo, B. Li, H. Sun, Q. Gu, H. Hao, Q. Shen, J. Wu, X. Liao,

S.P. Ringer, H. Liu, L. Zhang, W. Chen, F. Li and S. Zhang, The mechanism for the enhanced piezoelectricity in multi-elements doped (K,Na)NbO_3 ceramics, *Nat. Commun*. **12**, 881 (2021).

[17]J. Wu, D. Xiao and J. Zhu, Potassium-sodium niobate lead-free piezoelectric materials: Past, present, and future of phase boundaries, *Chem. Rev*. **115**, 2559 (2015).

[18]Q. Liu, J. F. Li, L. Zhao, Y. Zhang, J. Gao, W. Sun, K. Wang and L. Li, Niobate-based lead-free piezoceramics: A diffused phase transition boundary leading to temperature-insensitive high piezoelectric voltage coefficients, *J. Mater. Chem. C* **6**, 1116 (2018).

[19]Q. Liu, Y. Zhang, J. Gao, Z. Zhou, H. Wang, K. Wang, X. Zhang, L. Li and J. F. Li, High-performance lead-free piezoelectrics with local structural heterogeneity, *Energ. Environ. Sci*. **11**, 3531 (2018).

[20]X. Lv, J. Wu, D. Xiao, J. Zhu and X. Zhang, Electric field-induced phase transitions and composition-driven nanodomains in rhombohedral-tetragonal potassium-sodium niobate-based ceramics, *Acta Mater*. **140**, 79 (2017).

[21]B. Q. Ming, J. F. Wang, P. Qi and G. Z. Zang, Piezoelectric properties of (Li, Sb, Ta) modified (Na,K)NbO_3 lead-free ceramics, *J. Appl. Phys*. **101**, 054103 (2007).

[22]H. Tao, H. Wu, Y. Liu, Y. Zhang, J. Wu, F. Li, X. Lyu, C. Zhao, D. Xiao, J. Zhu and S. J. Pennycook, Ultrahigh performance in lead-free piezoceramics utilizing a relaxor slush polar state with multiphase coexistence, *J. Am. Chem. Soc*. **141**, 13987 (2019).

[23]S. Wada, H. Kakemoto and T. Tsurumi, Enhanced piezoelectric properties of piezoelectric single crystals by domain engineering, *Mater. Trans*. **45**, 178 (2004).

[24]P. Li, Z. Fu, F. Wang, Y. Huan, Z. Zhou, J. Zhai, B. Shen and S. Zhang, High piezoelectricity and stable output in $BaHfO_3$ and $(Bi_{0.5}Na_{0.5})ZrO_3$ modified $(K_{0.5}Na_{0.5})(Nb_{0.96}Sb_{0.04})O_3$ textured ceramics, *Acta Mater.* **199**, 542 (2020).

[25]W. Yang, Y. Wang, P. Li, S. Wu, F. Wang, B. Shen and J. Zhai, Improving electromechanical properties in KNANS-BNZ ceramics by the synergy between phase structure modification and grain orientation, *J. Mater. Chem. C* **8**, 6149 (2020).

[26]Y. Saito, H. Takao and T. Tani, Lead-free piezoceramics, *Nature* **432**, 84 (2004).

[27]P. Li, J. Zhai, B. Shen, S. Zhang, X. Li, F. Zhu and X. Zhang, Ultrahigh piezoelectric properties in textured (K,Na)NbO_3 -based lead-free ceramics, *Adv. Mater*. **30**, 1705171 (2018).

[28]Y. Chang, J. Wu, B. Yang, H. Xie, S. Yang, Y. Sun, S. Zhang, F. Li and W. Cao, Large, thermally stabilized and fatigue-resistant piezoelectric strain response in textured relaxor-$PbTiO_3$ ferroelectric ceramics, *J. Mater. Chem. C* **9**, 2008 (2021).

[29]K. Wang, F. Z. Yao, W. Jo, D. Gobeljic, V. V. Shvartsman, D. C. Lupascu, J. F. Li and J. Rödel, Temperature-insensitive (K,Na)NbO_3-based lead-free piezoactuator ceramics, *Adv. Funct. Mater*. **23**, 4079 (2013).

[30]F. Z. Yao, K. Wang, W. Jo, K. G. Webber, T. P. Comyn, J. X. Ding, B. Xu, L. Q. Cheng, M. P. Zheng, Y. D. Hou and J. F. Li, Diffused phase transition boosts thermal stability of high-performance lead-free piezoelectrics, *Adv. Funct. Mater*. **26**, 1217 (2016).